

## Development of a new experimental setup for studying collisions of keV-electrons with thick and thin targets

R K SINGH, R K MOHANTA, R HIPPLER\* and R SHANKER

Atomic Physics Laboratory, Physics Department, Banaras Hindu University, Varanasi 221 005, India

\*Fachbereich Physik, Universitaet Greifswald, Domstrasse 10a, 17487-Greifswald, Germany

Email: rshanker@banaras.ernet.in

MS received 13 February 2001; revised 20 August 2001

**Abstract.** Development of a new *electron-recoil ion/photon coincidence* setup for investigating some of the electron induced collision processes, such as electron bremsstrahlung, electron backscattering, innershell excitation and multiple ionization of target atoms/molecules in bombardment of electrons having energies from 2.0 keV to 30.0 keV with solid and gaseous targets is described. The new features include the use of a compact multipurpose scattering chamber, a time-of-flight spectrometer for detection of multiply charged target ions, a 45°-parallel plate electrostatic analyzer for measuring energy and angle of the ejected electrons, a room temperature high resolution Si-PIN photo diode X-ray detector for counting the collisionally induced photons, a coincidence data acquisition system consisting of a 200 MHz Pentium based 8K-multichannel analyzer and a standard network of a fast/slow coincidence electronics. In particular, the details of design, fabrication and assembly of indigenous components employed in the setup are presented. Selected experiments planned with the setup are mentioned and briefly discussed. A report on performance, optimization, efficiency, time resolution etc. of the time-of-flight (TOF) spectrometer and that of the 45°-parallel plate electrostatic analyzer (PPEA) is presented. Test spectra of electron-recoil ion coincidences, energy distribution of ejected electrons and characteristic plus non-characteristic X-ray spectrum are illustrated to exhibit the satisfactory performance of the developed setup.

**Keywords.** Time-of-flight spectrometer; parallel plate electrostatic analyzer; electron bremsstrahlung; electron backscattering; multiple ionization.

**PACS Nos** 07.81.+a; 34.80.Dp; 41.60.-m

### 1. Introduction

Collisions of electrons with atoms and molecules are one of the most fundamental interactions in nature. These interactions are basic to generate a variety of processes in different areas of physics, such as plasma physics (discharges and breakdowns, fusion, bremsstrahlung processes etc.), radiation physics (secondary electron effects, condensed-phase spur formation) and astrophysics (aurora borealis, planetary atmospheres, supernova activity). Ionization due to electron impact (EI) is also the most common form of ionization/multiple ionization in commercial mass spectrometers and is used as an analytical tool for measuring species concentrations in gaseous samples. However, reliable measurements

of EI ionization cross-sections, thick-target bremsstrahlung, electron backscattering and those of secondary electrons are lacking except for simple atoms and molecules. Cross-sections, in particular, for single ionization of the rare gases are generally regarded as well-known with independent measurements now agreeing to within 5–15% [1–3]. Recent measurements of singly differential cross-sections (SDCS) and doubly differential cross-sections (DDCS) for ejection of secondary electrons from atomic gases by electron impact have been reported [4,5]; but few sets of data exist for partial doubly differential ionization cross-sections [6]. In addition, much work has recently been done on ionization of atoms to higher charge states [7].

The bremsstrahlung spectra produced by electron bombardment of thick targets are important for knowing the process of penetration of electrons through matter. They are also of practical interest because of the widespread experimental and commercial use of X-rays and electron beams. X-ray spectra from medical X-ray units and from commercial X-ray tubes have been reported in the literature, but comparison of such spectra to theoretical models of thick target bremsstrahlung production is hindered by the large inherent filtration and fixed angles. The connection between the thick target and the thin target bremsstrahlung formulas requires a *comprehensive theory* on the passage of electron through matter. Recently, some work in this direction has been carried out in our laboratory on the measurement of absolute intensity and the doubly differential cross-sections for electron bremsstrahlung spectra at keV energies with thick targets [8–10]. The angular dependence of thick target bremsstrahlung spectra has been studied by Quarles and his coworkers [11] in the recent past.

The electron backscattering behaviour of solid targets, especially of thin films on bulk substrates is essential for applications in electron beam lithography, for micro fabrication of semiconductor chips, in scanning electron microscopy and for microprobe analysis. The backscattering process is also of value in the development of theories of bremsstrahlung production, cathodoluminescence, secondary electron emission, and bombardment induced conductivity. Very recently, we have measured the angular dependence of the backscattering coefficient from tungsten at electron impact energies of 3.0 keV and 5.0 keV [12].

Keeping in view the significance and the potential applications of electron interaction with solid and gaseous targets, we thought it worthwhile to develop a new experimental setup for making systematic studies of different collision processes, such as, the multiple ionization of atoms and molecules using a coincidence technique, the electron bremsstrahlung and the electron backscattering in the electron impact energy range of 2.0 keV to 30.0 keV. In this paper, we intend to describe the technical aspects of the experimental setup and details of design, fabrication and assembly of various indigenous components that are needed for measuring X-rays, secondary electrons and collision induced target ions. The study of performance, efficiency, precision involved with various components and that of the test results is conducted and reported.

It may be pointed out that this setup is the first of its kind in the country and is dedicated for analyzing X-rays, target ions and ejected electrons from atoms and molecules in energetic electron-atom/molecule collisions as a function of their emission angle and energy simultaneously using a coincidence technique at a chosen incident energy of electrons.

## **2. Design, fabrication and development of the experimental setup**

The experimental setup consists of the following major components:

- A compact scattering chamber
- A target handling system
- Faraday cup and charge measuring device
- High vacuum and pressure monitoring system
- A 50 keV electron gun
- A time-of-flight (TOF) spectrometer
- A 45°-parallel plate electrostatic analyzer (PPESA)
- Detectors (channel electron multiplier (CEM) and Si-PIN photodiode detector)
- A signal processing and data acquisition system

Description of each component is given in the respective subsections.

### *2.1 Compact scattering chamber*

A suitable scattering chamber has been designed and fabricated for the study of multiple ionization and bremsstrahlung photons generated from the interaction of energetic electrons with gaseous and solid targets. A schematic diagram of the chamber is shown in figure 1. The scattering chamber is a SS-cylinder of 216 mm height and 239 mm inner diameter. It has two collinear ports A, each fitted with a KF16 coupling; one adopts the electron gun via a differential pumping while the other one couples a Faraday cup. A detachable SS-plate B of 300 mm diameter and 12 mm thickness sits on top of the scattering chamber and can be sealed with a viton O-ring (diameter 242 mm). This plate is provided with two ports C each fitted with KF25 couplings, which adopt the pressure gauge heads. At the center of the top plate, a small circular SS-plate D of diameter 70 mm and thickness 5 mm is fitted, which contains two ports to facilitate the mounting of target gas inlet and outlet. The target gas inlet can be either attached with a hypodermic needle or with a gas cell E. The small plate D can be replaced by a movable target holder assembly for mounting the solid targets. This arrangement permits a proper positioning of the solid targets without cycling the vacuum of the system. The bottom plate F of scattering chamber is a SS-plate of 300 mm diameter and 12 mm thickness. Center of this plate is fitted with a SS-cylinder of 109 mm length with CF100 flange G. Flange G adopts a SS-cylinder of 80 mm length with a CF100 to ISO 100 transition coupling (not shown in the figure). The ISO 100 flange directly couples a turbo molecular (TM) pump. Further, a SS-plate H of 150 mm diameter and 5 mm thickness is fixed on the bottom plate (F) of the scattering chamber. There are several holes in plate H for evacuating the scattering chamber. An aluminum cylindrical stand I and a circular-rotating disc J are co-axially fixed at the center of the plate H. A cylindrical stand holds the hypodermic needle assembly or the gas cell (E) for providing the gaseous targets. A stand K is mounted on the rotating disc to hold the PPEA and the CEM. This arrangement facilitates the rotation of PPEA and CEM around the collision center by a remote control device L, with an accuracy of  $\pm 0.5^\circ$ .

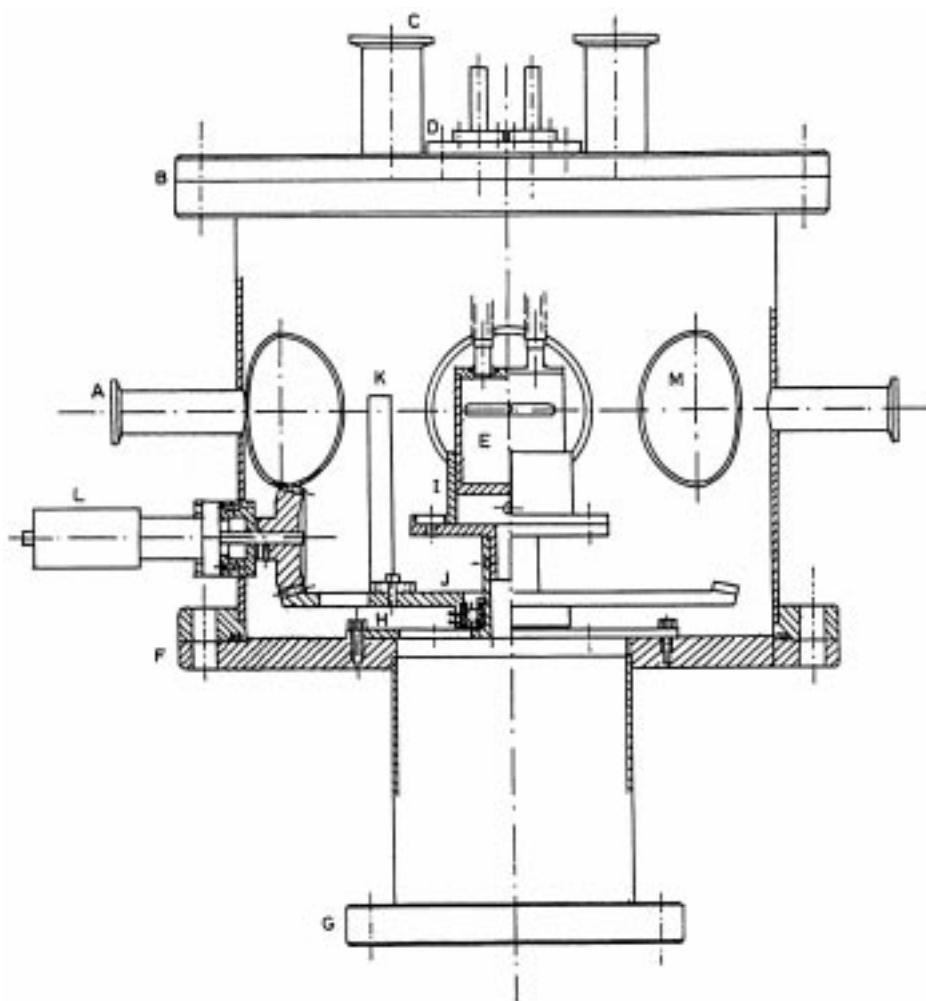


**Figure 1.** Cross-sectional view of the main scattering chamber. Meaning of various alphabetical symbols appearing in the figure are described in the text.

There are five additional ports M on the vertical wall of the scattering chamber, each is fitted with a ISO-70 flange which are positioned at  $+30^\circ$ ,  $+90^\circ$ ,  $-135^\circ$ ,  $-60^\circ$  and  $+120^\circ$  with respect to the electron beam direction. The centers of each port, the level of electron beam and the collision center all lie in the same horizontal plane. A special adapter has been constructed to insert the Si-PIN photodiode X-ray detector very close to the collision center. This adapter can be fitted on any one of the five ports. It allows the Si-PIN photodiode detector to look through a 5 mm hole situated on the end cap of the detector. In the present configuration, one of the five ports is used to serve as a 'viewing port' and two others are used to carry electrical connections from CEMs, TOF and PPEA units. Five BNCs and one SHV connectors are fixed on each flange of these ports with araldite to meet the above purpose.

## 2.2 Target handling system

2.2.1 *Gas beam using a hypodermic needle:* A hypodermic needle ( $\phi \sim 1$  mm and length 30 mm) or a multicapillary tube is mounted on an aluminium hollow cylinder having 90 mm length, 50 mm outer diameter and 4 mm wall thickness (see figure 2). The cylinder was machined in such a way that on one hand, it allows the electron beam to traverse through two collinear holes of 8 mm diameter in a horizontal plane; on the other hand, it allows the gas beam to emanate from the hypodermic needle which crossfires the electron beam at  $90^\circ$  in the center of the scattering chamber. The target gas is put into the collision zone through a teflon tubing attached to the hypodermic needle. Provision is made to move the needle's tip up or down for its proper alignment with respect to the electron beam. A horizontal flat aluminium platform of dimensions  $130$  mm  $\times$   $39$  mm  $\times$   $1$  mm is attached to the above cylinder for mounting the TOF and the CEM on it. The lower tip of the hypodermic needle can be placed in between the two electrodes  $P_+$  and  $P_-$  of the TOF (see figure 3). The CEM of the TOF spectrometer is sandwiched between the two vertical plates fixed on the platform, which provides a provision to move the CEM along the axis of TOF towards or away from the latter. A hole of 10 mm diameter is drilled in the platform just below the hypodermic needle to finally pump down the target gas by a TM pump placed underneath. The whole system sits on a hollow cylindrical stand of the scattering chamber (see subsection 2.1). This stand facilitates the aluminium cylinder to move up or down for its alignment with respect to the electron beam.

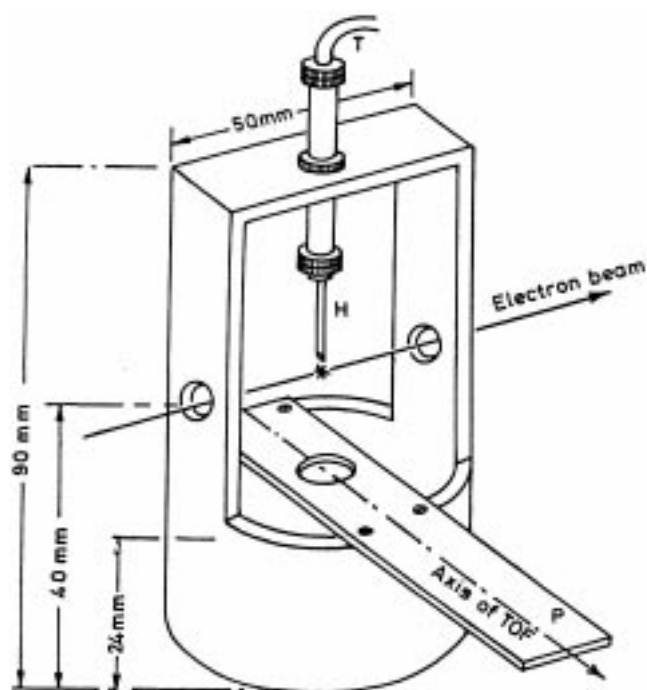


**Figure 2.** Schematic diagram of the hypodermic needle assembly. T: teflon tube; H: hypodermic needle; P: platform for mounting the TOF and the CEM.

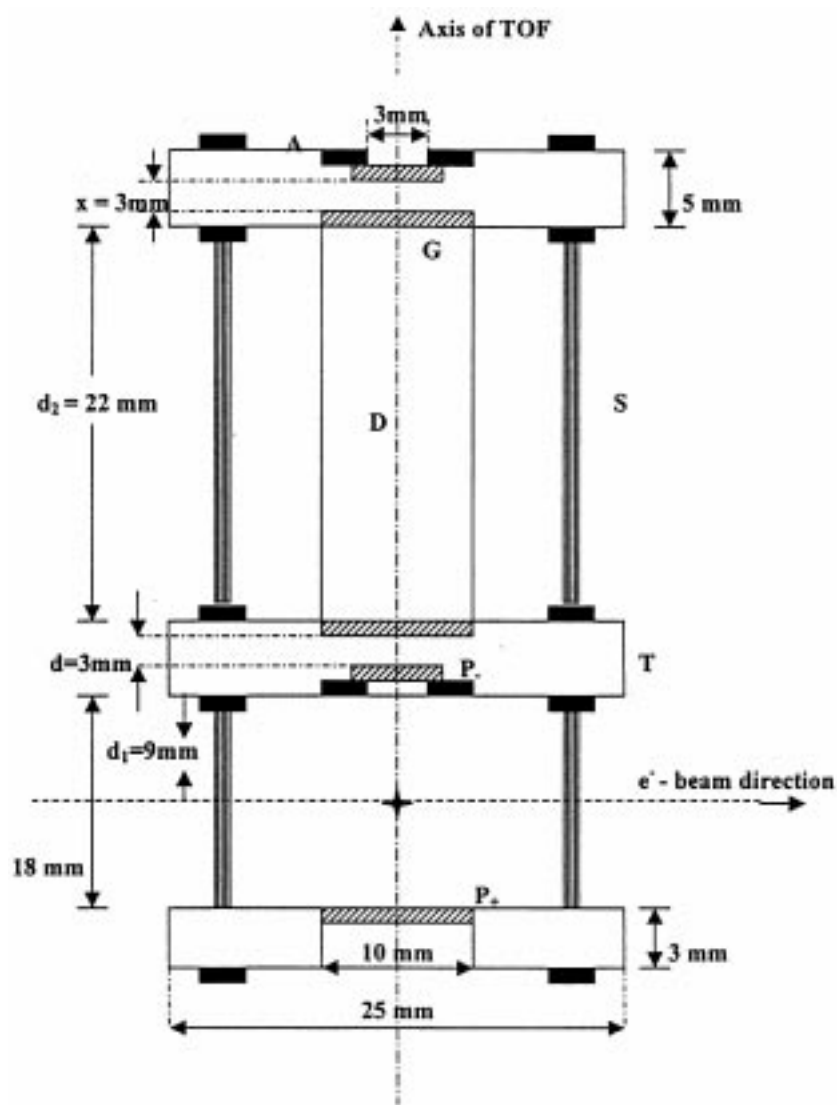


**Figure 3.** Principle diagram of a TOF spectrometer.  $P_+$  and  $P_-$  : extracting electrodes for electrons and ions, respectively; D: drift tube; G: SS grid; A: accelerating plate; T: teflon ring; S: SS rod.

2.2.2 *Gas cell:* A cylindrical gas cell having an identical diameter as that of the Al-cylinder (hypodermic assembly) but of height 60 mm, is needed for determining the cross-sections of reaction products on *absolute scale* as well as for studying the atomic field bremsstrahlung from gaseous targets. The bottom of the gas cell is closed while the upper end is provided with two ports for inlet and outlet of the target gas. It has two collinear

holes of 8 mm diameter through which the collimated electron beam passes and traverses the gas cell. A slot of 5 mm height is cut in the cylinder on one side of the collinear ports in a horizontal plane containing electron beam and the axis of Si-PIN photodiode detector (see figure 1). The slot is covered with a 6  $\mu\text{m}$  thick hostaphan foil. The target gas is introduced in the cell through a teflon tubing attached with an inlet port of the cell. The adjustment of the input gas pressure in the cell is done by a fine needle valve (Balzer-EVNO10 HI) in such a way that a *single collision condition* is maintained in the gas cell. The pressure of the gas cell is measured on an absolute scale by a MKS Baratron membrane manometer (model-127aa-00001D).

*2.2.3 Mounting of the solid targets:* A vacuum tight movable target holder (a SS-shaft of 10 mm diameter) is mounted at the center of an aluminium plate of 70 mm diameter and 5 mm thickness. When one wishes to use a solid target, this plate together with the target holder replaces the identical plate used earlier for gas targets (see subsection 2.1). Thin self-supporting foils of desired elements are mounted on an aluminium frame having four consecutive holes each of 12 mm diameter. The frame is attached to the SS-shaft through an insulator. This arrangement enables the positioning of the foil at a desired place and at a desired angle in the center of the chamber without cycling the vacuum in the system (for details, see ref. [13]).

### *2.3 Faraday cup*

A Faraday cup is a device to collect the charge of the transmitted electron beam through the target. In our setup, it consists of a hollow SS-cylinder of 75 mm length and 10 mm inner diameter and it is snugly fitted over a copper tube of length 6 mm and inner diameter 9 mm. A teflon ring of 16 mm diameter fitted over the SS-cylinder is connected to a SS-tube of 100 mm length which finally couples with the scattering chamber. This teflon ring holds the cylinder in a horizontal plane and it is properly insulated from the scattering chamber. The output signal from the copper cylinder is taken out through a BNC connector.

### *2.4 High vacuum and pressure monitoring system*

The main scattering chamber is evacuated by a combination of a TM pump (TPH-240, Inlet-DN-100 ISO, 240 l/s) and a fore-pump (E2M8, 8.2  $\text{m}^3/\text{h}$ ), while the electron gun enclosure by a TM pump (TPU-062, Inlet-DN-63CF, 52 l/s) and a fore-pump (E2M5, 5 $\text{m}^3/\text{h}$ ). The pressures maintained by the pumps are measured by two compact full range dual gauge heads: PKR 251 (Pirani and cold cathode gauges) coupled with their respective control units. TM pumps and pressure measuring devices were purchased from M/S Balzer Pfeiffer GmbH, Germany, while the fore-pumps were obtained from M/S Edward High Vacuum Instrumentation, UK. The stabilized powers to TM pumps and to their controllers were given through a 5 kW Servo Stabilizer and to fore-pumps through a 3 kW AVS. The base pressure of the scattering chamber and that of the electron enclosure are found to be better than  $1.6 \times 10^{-6}$  torr.

## 2.5 50 keV electron gun

In the present setup, we are using a custom built electron gun, model EK-50-H.V. with required high voltage power supply (M/S STAIB Instruments, Germany). This electron gun has been developed specially for high beam energy applications. All electrical requirements, i.e., filament current, grid voltage, focusing voltage and deflecting voltage are supplied by a single compact 50 kV power supply (NEK-50-HD). The deviation unit, which is an electromagnetic coil, can be rotated freely around the gun axis. A remote box with a 4-m cable controls X-Y deflecting, focusing and grid voltages. Beam energy can be varied between 2 keV and 30 keV with an accuracy of 1%. The beam spot lies between  $50\ \mu\text{m}$  to 3 mm depending upon the working distance (10–100 cm) from the mounting flange of the electron gun.

**2.5.1 Coupling of electron gun with scattering chamber:** The electron gun is coupled with the main scattering chamber through a standard 'cross' having CF35 flanges (see figure 4). In order to keep the electron gun under vacuum while not in use, a gate valve (M/S VAT Vakuumentile, Switzerland) is interposed between TM pump and the electron gun through CF35 couplings. The opposite flange of the gate valve is coupled with one of the horizontal ports of the cross. The other end of the cross couples the main scattering chamber through a reducer, CF35 to KF16. The vertical upper port of the cross is coupled with a 25 cm long

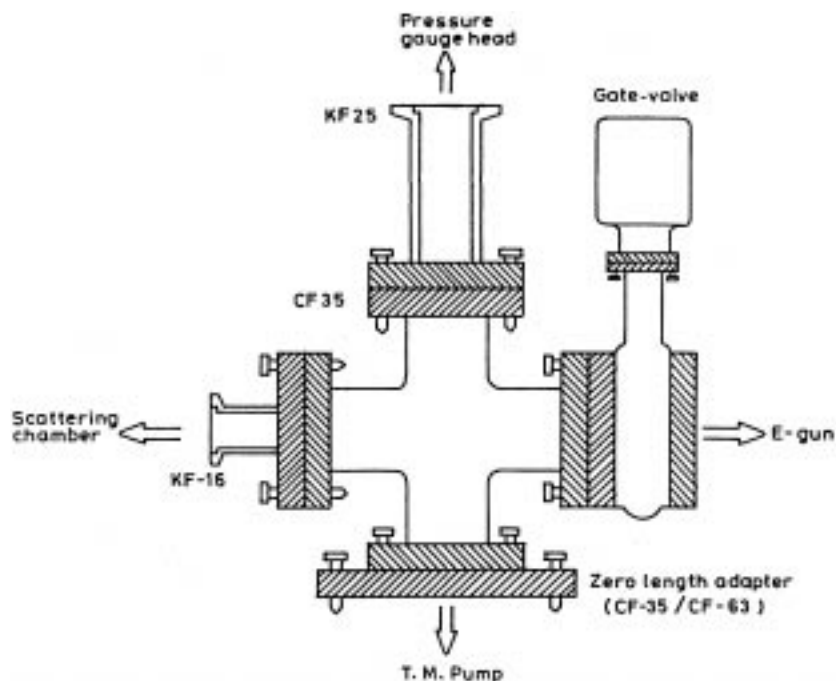


**Figure 4.** Schematic diagram of the 'CROSS' showing the coupling arrangement of gate valve, pressure gauge head, turbo-molecular pump and main scattering chamber.

reducer (CF35 to KF25) for mounting a pressure gauge head. A large separation between the beam path and the gauge head is necessary because the magnetic field caused due to the gauge head may influence the collimation of the electron beam. Lower port of the cross is attached with a zero length adapter (CF35 to CF63). The CF63 flange directly couples the TM pump (TPU-062) for evacuating the electron gun enclosure.

### *2.6 Time-of-flight (TOF) spectrometer*

Interaction of fast moving electrons with neutral gaseous atoms results in ejection of a large number of electrons from the target. Various charge states of the ionized target atoms (multiply charged ions) can be separated on the basis of their times of flight over a certain path length, because the time of flight  $T$  of the ions of mass  $m$  and charge state  $q$  is proportional to the square root of  $m/q$ . Thus, when the ions reach the TOF detector, they are separated into bunches; each bunch corresponding to a certain value of  $m/q$ , or a specific charge state of the target ion.

A schematic diagram of the TOF setup is shown in figure 3. It has an interaction zone enclosed between two electrodes,  $P_+$  and  $P_-$ , where the electron beam crosses a beam of neutral gaseous atoms effusing from a hypodermic needle.  $P_+$  is the SS-grid (transparency 80%) of circular form of diameter 10 mm through which the ejected electrons pass and may enter into the PPEA.  $P_-$  is the SS-circular disc of diameter 10 mm. The separation between  $P_+$  and  $P_-$  is 18 mm. A positive voltage on the  $P_+$  and an equal negative voltage on the  $P_-$  help in pulling out the electrons and ions respectively from their birthplaces in the opposite directions. A 3 mm hole in  $P_-$  electrode provides a passage for the ions to come out from the interaction zone. The hole is covered with a SS-grid of parallel wires having 80% transmission efficiency for maintaining the uniform electric field. Once out of the hole, the ions are accelerated over a distance  $d$  (3 mm) before they enter an aluminium drift tube  $D$  of length 22 mm and diameter 10 mm. After coming out from the drift tube, ions are accelerated over a distance  $x$  (3 mm) and pass through a 3 mm hole of the last accelerating plate  $A$ . The accelerating plate  $A$  is a SS-disc of 10 mm diameter; it is kept at about  $-800$  V which provides enough kinetic energy for ions to impinge the cone of the CEM. The two ends of drift tube and hole of the plate  $A$  are again covered with grids of similar transmission as mentioned above. The assembly of plates, grids and drift tube is fixed on a series of teflon rings of diameter 24 mm. Teflon rings are aligned with the help of three SS-rods of 3 mm diameter. The rods are fixed in the rings at  $120^\circ$  from each other. A more detailed description of a similar TOF spectrometer can be found in our earlier work [14].

### *2.7 $45^\circ$ -Parallel plate electrostatic analyzer (PPEA)*

Electrostatic energy analyzer works on the principle that the path of a charged particle in an electric field is dependent on the particle's energy. The simplest analyzer consists of two parallel plates held at different potentials, thereby creating a uniform electric field between them. The charged particles that enter this field at  $45^\circ$  at the entrance slit, follow a parabolic path and are refocussed at the exit slit of the analyzer. According to their initial kinetic energy, those particles which are able to pass through the exit slit are detected. There is

a linear relationship between the voltage applied between the plates and the energy of the particles which are able to pass through both slits [15].

The schematic diagram of a PPEA is shown in figure 5. The front plates F are made from SS and have dimensions  $100\text{ mm} \times 40\text{ mm} \times 3\text{ mm}$ . The entrance and exit slits are  $4\text{ mm}$  wide and  $10\text{ mm}$  in height and they are separated by a distance of  $70\text{ mm}$ . The distance between front and back plates is  $21\text{ mm}$ . These relatively wide slit widths are chosen so as to give a moderate energy resolution ( $\Delta E/E$ ) of about 12% for a better transmission efficiency. In the case of low energy electron beam experiments, additional elastically scattered peak is also sometimes observed with the main elastic peak. This peak is due to the reflection of the low energy electrons (or ions) compared to the main elastic peak. These reflected low energy electrons from the back plate B are eliminated by adding two intermediate plates between the two end plates with an equal spacing between each other. Trajectory calculations can be made to determine the exact electron path under the influence of the electric field, so as to make apertures at the precisely right places in each of these intermediate plates. The two end plates along with intermediate plates are electrically insulated from each other by precision-machined teflon tubular supports.

For the energy analysis of electrons, the negative voltage is given to the back plate while the front plate is grounded; each of the intermediate plates between the front and back plates of the analyzer are connected by a resistance chain so as to provide a linear voltage gradient and thus create a uniform electric field. The PPEA has been designed and fabricated for us by M/S Sairam, Mumbai. A test spectrum of the energy distribution of ejected electrons using the PPEA at  $90^\circ$  to the electron beam direction in  $8.0\text{ keV } e^- - \text{Ar}$  collisions is shown in figure 6. In this figure, the peak appearing at about  $200\text{ eV}$  arises due to the initial vacancy created in the L shell of argon and being filled by emission of Auger electrons.

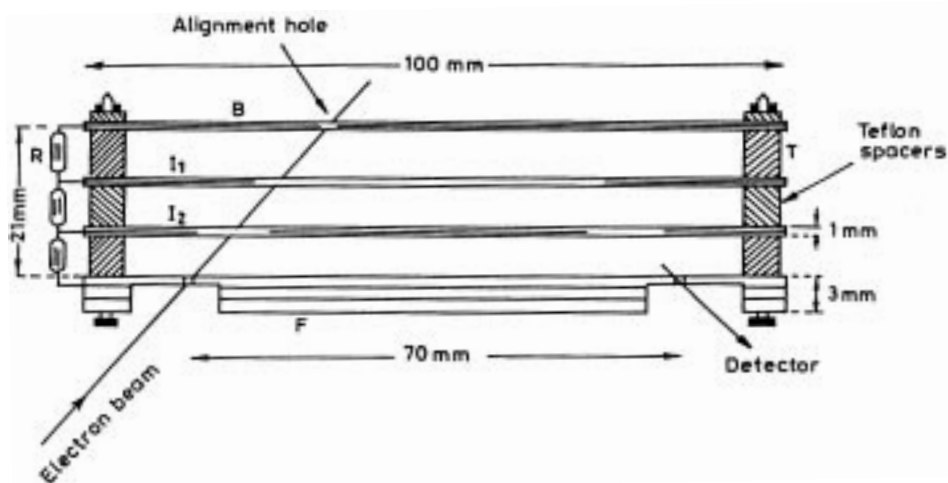


**Figure 5.** Schematic diagram of a  $45^\circ$ -parallel plate electrostatic analyzer.  $I_1$  and  $I_2$ : intermediate plates, R: resistance chain; T: teflon spacers; B: back plate; F: grounded plate.

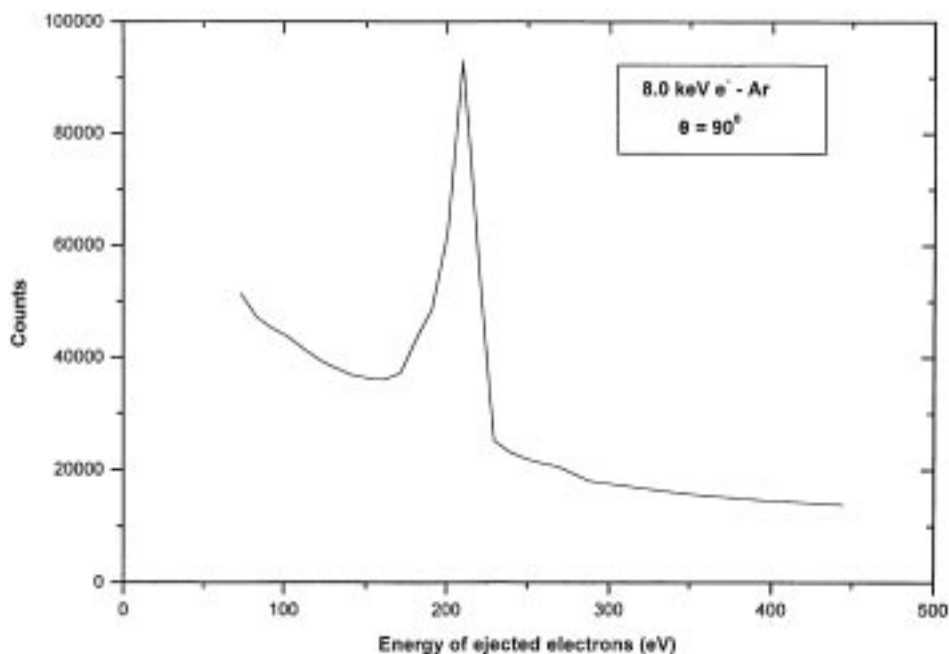


**Figure 6.** The energy distribution of ejected electrons at  $90^\circ$  to the electron beam direction in 8.0 keV  $e^-$ -Ar collisions.

## 2.8 Detectors

For performing the multiple ionization experiments, one needs fast timing detectors for obtaining a reasonably good charge separation of the multiply charged ions. Both the micro channel plates (MCP) and the CEM can be used for this purpose. MCPs have better time resolutions than CEMs but they are fragile and need special care to handle, so we preferred to use two CEMs (model-MD-501, M/S AMPTEK Inc., USA) for detecting electrons and ions. The model MD-501 is a unit of compact design (dimensions: 83 mm  $\times$  57 mm  $\times$  19 mm) provided with a high voltage converter and a charge sensitive preamplifier and has several attractive features. For example: handling count rate  $\sim 10^6$  cps; pulse pair resolution  $\sim 250$  ns; gain  $\sim 10^7$ ; electrical requirements +10 V to +15 V, 30 mA (depending upon the supply voltage); operating pressure  $\leq 1.0 \times 10^{-4}$  torr.

Generally, the conventional X-ray solid state detectors, e.g., a Si(Li), HPGE and Ge(Li) are not convenient to use due to their large sizes and requirements of liquid nitrogen for their cooling. So, we have chosen to use a high resolution, thermoelectrically cooled Si-PIN-photo diode as an X-ray detector equipped with a charge sensitive preamplifier (model XR-100T, dimensions 95 mm  $\times$  44 mm  $\times$  29 mm, M/S AMPTEK Inc., USA), which can be operated at a normal room temperature. Power to the XR-100T is provided by the PX2T power supply which is a.c. powered and includes a spectroscopy grade shaping amplifier. Energy resolution (FWHM) of this detector is 180 eV at 5.9 keV at room temperature.

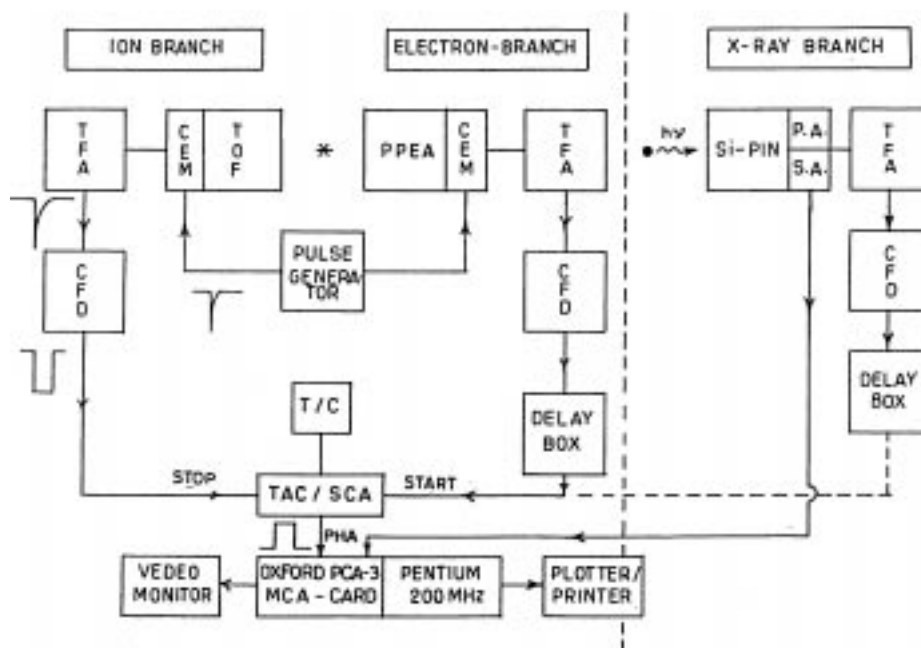


**Figure 7.** Block diagram of the electronic-circuits employed for processing signals in carrying out multiple ionization, electron and X-ray measurements. TFA: timing filter amplifier; CFM: constant fraction discriminator; T/C: timer/counter; TAC/SCA: time-to-amplitude converter/single channel analyzer; PHA: pulse height analyzer; PPEA: pre-amplifier; SA: spectroscopy amplifier.

## 2.9 Signal processing and data acquisition system

A block diagram of various electronics modules used in processing electron, ion and photon signals is shown in figure 7. Standard NIM modules are used to process electronic signals generated by the channeltrons and the X-ray detector. For multiple ionization experiments, two channeltrons are employed: one to detect the target ions and the other to detect the ejected electrons in coincidence. The output signals of these channeltrons are fed to a Quad timing filter amplifier, TFA (model-863, Ortec) and then into a constant fraction discriminator, CFM (model-TC 454, Oxford Instr.). CFM produces fast negative NIM pulses which are fed as 'START' and 'STOP' inputs to a time-to-amplitude converter, TAC (model-TC-863, Oxford Instr.). In our experiments, the ion signals derived from the TOF spectrometer is used as a STOP signal while the electron signals derived from PPEA as a START signal to the TAC. An Oxford window-based MCA (multi-channel analyzer) software and Oxford PCA-3, 8K-MCA card are installed in our computer (Pentium-200 MHz). The data acquisition, management, stripping and plotting etc. are made possible by interfacing the experiment with the above mentioned MCA.

In electron bremsstrahlung measurements, X-ray photons are detected by a Si-PIN photo-diode detector. The output of the detector is fed into the MCA input through various modules (described above) for the data acquisition.

In all the above mentioned experiments, the monitoring of electron beam current is accomplished by a pico-ammeter and the integration of electronic charges is done by a current integrator (EG&G, Ortec 439) for normalization purposes.

### 3. Planned experiments with the setup

- Measurement of partial doubly differential cross-sections of ions produced in collisions of 2.0 keV–30.0 keV electrons with atoms and molecules.
- Energy and angular distributions of electrons ejected from gaseous targets by keV electrons.
- Angular distribution of electron bremsstrahlung photons in keV-electron collisions with solid and gaseous targets.
- Electron backscattering studies from solid targets including thin films.

#### 3.1 Measurement of partial doubly differential cross-sections of ions produced by impact of 2.0 keV–30.0 keV electrons with atoms and molecules

Multiple ionization of atoms, as a result of charged particle impact or photon impact is a complex phenomenon and has no complete mathematical formulation till date. Data are available for single differential cross-sections (SDCS) and doubly differential cross-sections (DDCS) for multiple ionization of some atomic and molecular gases, but very few sets of data exist for partial doubly differential ionization cross-sections. So, we have planned to make a reliable and a systematic experimental study of partial doubly differential ionization cross-sections of inert gas atoms, for example, He, Ne, Ar, Kr and Xe in coincidence with ejected electrons of known energy and angle of emission.

We are interested in studying the partial doubly differential cross-sections for the collision reaction



where  $X$  is an atom of helium, neon, argon, krypton or xenon and  $n$  is the charge state of ion produced. Detection of one of the slow electrons (ejected from the target atoms) in coincidence with the product  $X^{n+}$  ions enables one to identify a particular  $n$ -fold ionization process. Experimentally, partial doubly differential cross-sections for  $n$ -fold ionization can be measured by using the relation

$$d^2\sigma^{(n)}/dE d\Omega = N_c^{(n)}\sigma_i/[N_i\Delta E \Delta\Omega \varepsilon], \quad (2)$$

where  $N_c^{(n)}$  is the number of true coincidence counts for  $n$ -fold ionization,  $N_i$  is the number of detected ions,  $\varepsilon$  is the efficiency of detection system,  $\sigma_i$  is the total cross-section for multiple ionization and  $\Delta E$  and  $\Delta\Omega$  are respectively the energy band width and the solid angle of the electrostatic analyzer.

3.1.1 *Experimental procedure:* A well collimated electron beam cross-fires a beam of atomic gas effusing from a hypodermic needle. Ejected electrons from the interaction

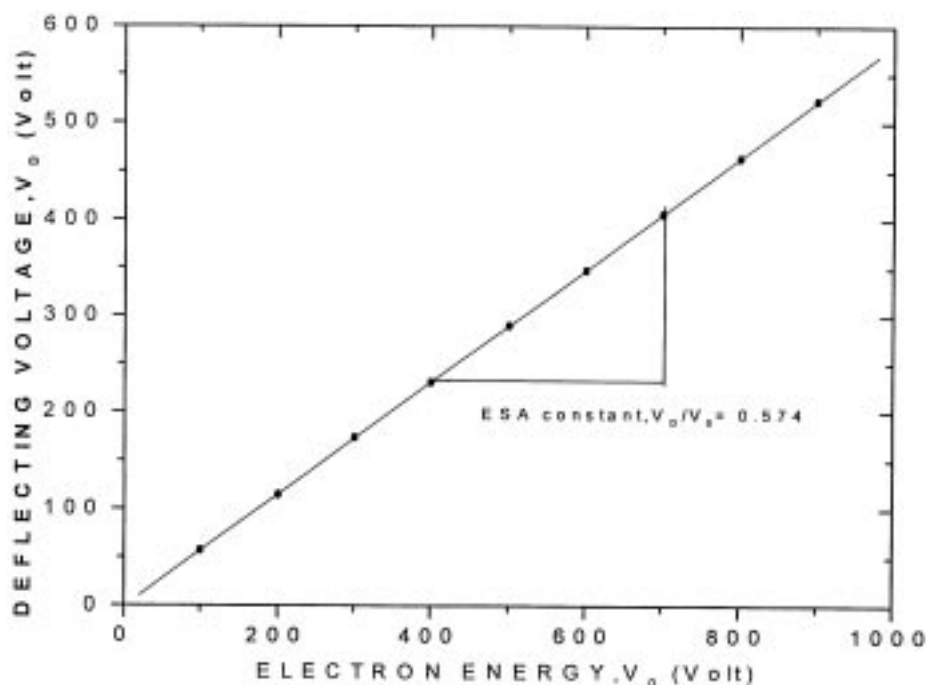


**Figure 8.** Deflection voltage  $V_D$  applied to one of the plates of PPEA versus energy of incident electrons  $V_0$ .

region are accepted with a narrow solid angle by a  $45^\circ$  parallel plate electrostatic analyzer positioned at different angles with respect to the electron beam direction and finally detected by a channeltron. Ions produced in the collision process are extracted by a small electric field ( $\sim 160$  V/cm) applied between the two plates  $P_+$  and  $P_-$  of the TOF spectrometer (see figure 3). Inside the TOF, ions are further accelerated and finally detected by a CEM as discussed in subsection 2.6. Both ion and electron signals coming from respective CEMs are processed with different NIM modules and a coincidence time spectrum is recorded in the MCA as described in subsection 2.9. The time delay between the arrival of ejected electrons and that of product ions at the respective CEMs gives information about the charge state of the ions.

Some results on the optimization of various components involved in measurement of multiple ionization process in keV-electron collisions with a dilute argon gas using the coincidence technique have been obtained. These are listed as follows:

- (1) Deflection voltage  $V_D$  applied to one of the plates of PPEA versus energy of incident electrons  $V_0$ ; this gives the value of constant of PPEA = 0.574 (see figure 8).
- (2) Width of response of the PPEA to electrons having a single energy  $V_0$  as a function of  $V_0$ ; this gives the energy resolution of the PPEA = 2% with entrance and exit slit widths each = 1 mm (see figure 9).
- (3) Variation of argon gas pressure as a function of  $\text{Ar}^+$  ion counts for ensuring a 'single collision condition' the operating pressure is chosen to be about  $2.4 \times 10^{-4}$  torr (see figure 10).

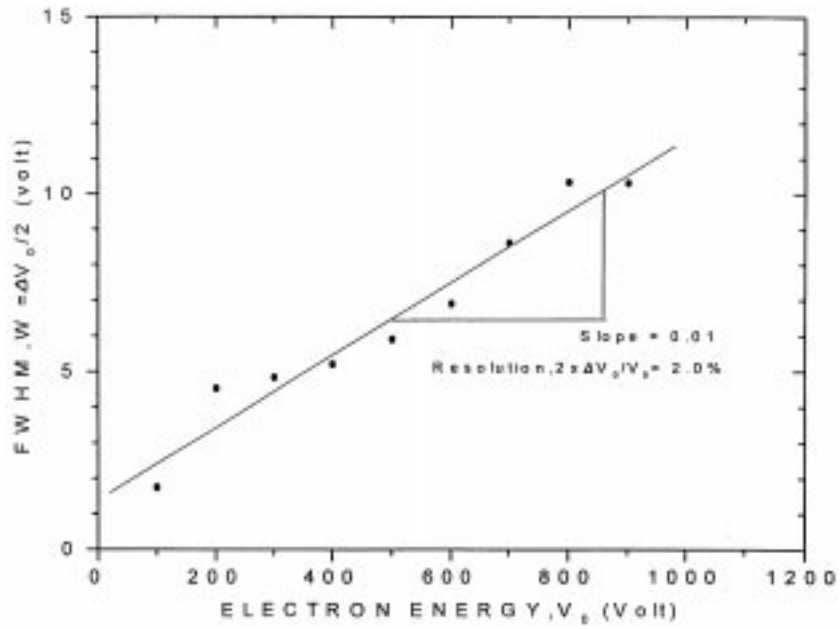


**Figure 9.** Width of response of the PPEA to electrons having a single energy  $V_0$  as a function of  $V_0$  with entrance and exit slit widths each equal to 1 mm.

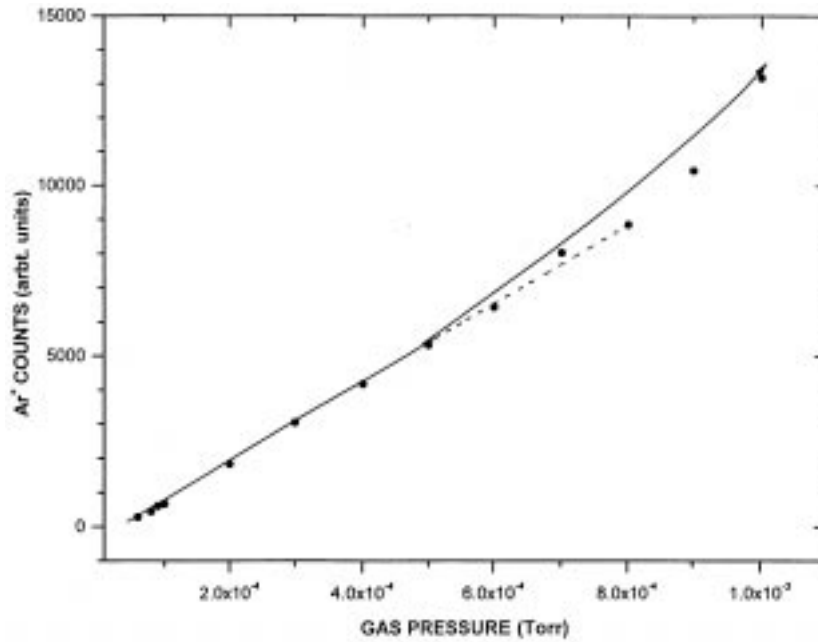


**Figure 10.** Variation of argon gas pressure as a function of  $Ar^+$  ion counts for ensuring a 'single collision condition'.

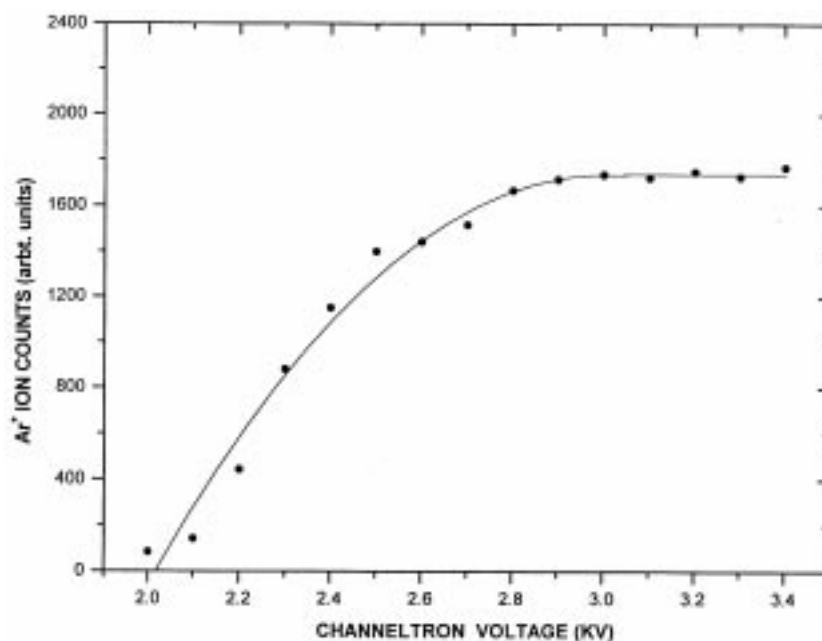


**Figure 11.** Variation of bias voltage of channeltron detector for TOF spectrometer as a function of  $\text{Ar}^+$  counts for ensuring detection of all ions having various charge states with equal efficiency.

- (4) Variation of bias voltage of channeltron detector for TOF spectrometer as a function of  $\text{Ar}^+$  counts for ensuring detection of all ions having various charge states with equal efficiency; the operating bias voltage is chosen to be 2.9 kV (see figure 11).
- (5) Variation of  $\text{Ar}^+$  ion counts versus ion-extraction voltage for our TOF spectrometer; the optimum ion extraction voltage is found to be beyond  $-160$  V for all ions of different charge states with equal transmission at a post acceleration voltage of  $-800$  V. The CEM mouth voltage is  $-2.9$  kV (see figure 12).
- (6) A typical TOF spectrum of  $\text{Ar}^{n+}$  ions ( $n = 1-6$ ) obtained by making coincidences between ions with ejected electrons of all energies at  $90^\circ$  with respect to the incident electron beam direction in  $20.0$  keV  $e^-$ -Ar collisions in a single collision condition is shown in figure 13. The typical time resolution obtained in the experiment is about  $10$  ns for  $\text{Ar}^{4+}$  ions.

### 3.2 Angular distribution of electron bremsstrahlung photons in keV – Electron collisions with solid and gaseous targets

Atomic field bremsstrahlung (AFB) is the radiation of photons emitted in the scattering of an electron from an atom or ion. The phenomenon of electron bremsstrahlung in the Coulomb field of an atom can be represented by the following equation:

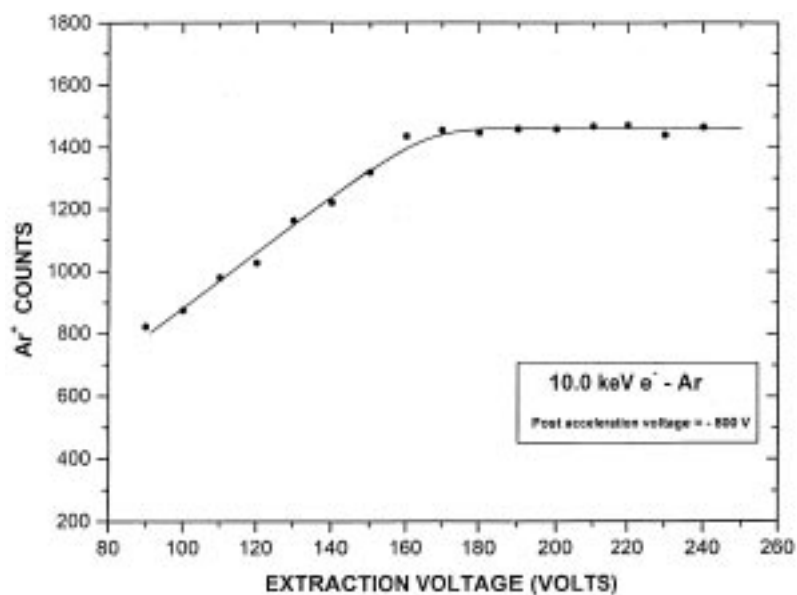


**Figure 12.** Variation of  $Ar^+$  ion counts as a function of ion-extraction voltage at a post acceleration voltage of  $-800$  V. The CEM mouth voltage is kept at  $-2.9$  kV.

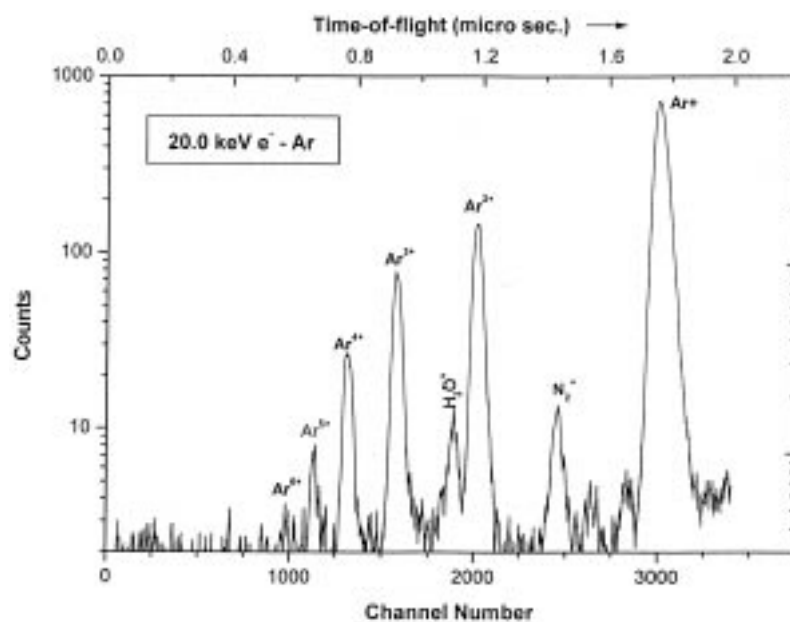


**Figure 13.** A typical TOF spectrum of  $Ar^{n+}$  ions ( $n+ = 1-6$ ) obtained by making coincidences between ions with ejected electrons of all energies at  $90^\circ$  with respect to the incident electron beam direction in  $20.0$  keV  $e^-$ -Ar collisions in a single collision condition. A typical time resolution obtained is  $10$  ns.

$$e_i^- + \text{atom} \rightarrow e_s^- + \gamma + \text{atom (unchanged)}, \quad (3)$$

where  $\gamma$  represents the emitted photon,  $e_i^-$  and  $e_s^-$  are incident and scattered electrons, respectively. The energy of photon is represented in terms of wave number  $k$  ( $k = 2\pi/\lambda = |\mathbf{k}|$ , where  $\mathbf{k}$  is a wave vector).

Investigations of the electron bremsstrahlung spectra may be grouped into two categories: (i) the targets are sufficiently thick to stop all the incident electrons, i.e., the targets may be foils (solid targets) which are thin enough to transmit a substantial fraction of X-rays but sufficiently thick to arrest all the incident electrons and (ii) the targets are extremely thin (gaseous targets) in order to allow the electrons to pass through with only a very small number of interactions. In the present setup, we have planned to study the angular distribution of AFB from both solid and gaseous targets and calculate the absolute and relative DDCS to provide additional experimental data for AFB at keV energies for testing the existing theories for semi thick and thin targets. The experimental absolute doubly differential cross-sections for the *thin* targets can be written as

$$d^2\sigma/dk d\Omega = N_B(k)/[N_e N_t \varepsilon(k) \Delta k \Delta\Omega], \quad (4)$$

where  $N_B(k)$  is the number of bremsstrahlung photon counts at a particular photon energy  $k$  in energy window  $\Delta k$ ,  $N_e$  is the total number of incident electrons,  $N_t$  is the number of target atoms/cm<sup>3</sup>,  $\Delta\Omega$  is the solid angle of photon detector and  $\varepsilon(k)$  is the detector efficiency. Equation (4) is also applicable for the thick targets with the correction of electron energy loss, electron backscattering and photon attenuation using a modified Kramers–Kuhlenkampff–Dyson (KKD) formula [16].

**3.2.1 Experimental procedure:** (i) *Solid targets:* The scattering chamber and electron gun are evacuated to provide a base pressure of the system of about  $1 \times 10^{-6}$  torr. The chamber is equipped with a movable target holder in the vertical plane at its center, which facilitates the positioning of targets in front of the beam. A high purity thin foil of targets are mounted on the target holder. The photon emitted from the beam target interaction zone passes through a  $6 \mu\text{m}$  hostaphan vacuum window in the horizontal plane and finally strikes the X-ray detector. The detector can be placed at a chosen angle with respect to the incident beam direction. The photon signals generated by the detector are amplified, shaped and digitized. Accumulation of the desired AFB spectra for a chosen angle and incident energy is carried out on a window based MCA in PHA mode. The incident electron beam is monitored on the insulated target for normalization purposes.

(ii) *Gaseous targets:* A gas cell as described in subsection 2.2.2 is used to study the gaseous targets. The pressure of the gas is measured by a MKS capacitance manometer. The ‘single collision condition’ is ensured by measuring the linear dependence of the gas pressure as a function of bremsstrahlung photon counts in a chosen energy window  $\Delta k$  per incident electron for a given energy of impact. This ‘thin’ target ensures that the multiple scattering events are negligible. The incident electron beam is monitored on the Faraday cup (see subsection 2.3). A typical x-ray spectrum produced in collisions of 14.0 keV electrons with a dilute argon gas at  $90^\circ$  to the electron beam direction is shown in figure 14. The spectrum shows clearly the characteristic peak of Ar–K at about 3.0 keV and the continuous bremsstrahlung background underneath.

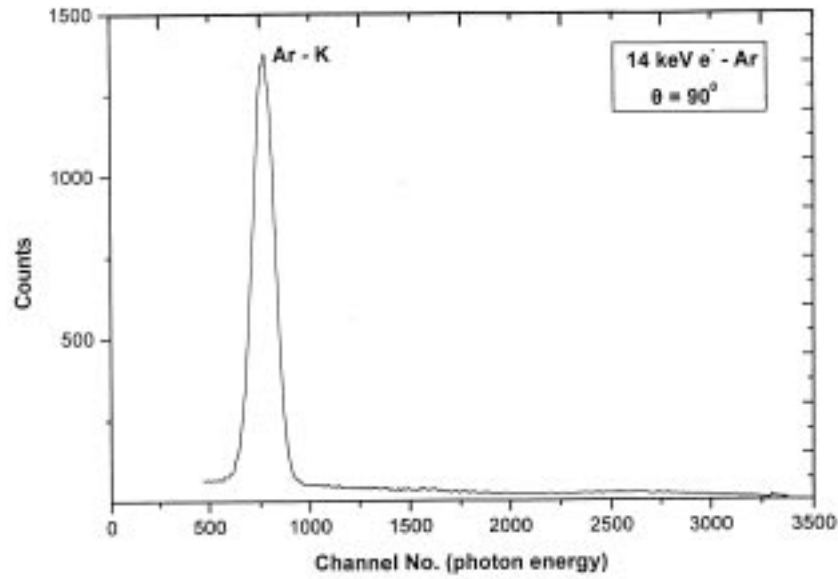


**Figure 14.** X-ray spectrum produced in collisions of 14.0 keV electrons with a dilute argon gas at  $90^\circ$  to the electron beam direction.

### 3.3 Electron-backscattering from solid targets

Backscattered electrons refer to those electrons which have energies  $> 50$  eV and are scattered through more than  $90^\circ$ , when electrons of higher incident energy (say, a few keV) are directed towards a solid target. A backscattering coefficient ' $\eta$ ' is defined as the ratio of intensity of the backscattered electrons ( $i_b$ ) and the intensity of the incident primary electrons ( $i_p$ ), i.e.,  $\eta = i_b/i_p$ . The results obtainable for the backscattering coefficient  $\eta$  for higher atomic numbers at low impact energies in the literature are scarce and there are considerable inconsistencies among the reported works. We, therefore, plan to look into these inconsistencies more closely and conduct more precise experimental study of energy and angular dependence of backscattering coefficient and also of secondary electron emissions from solid targets (specially for high  $Z$ ) with the present set up.

The secondary emission yield  $\delta$  is the ratio of the number of secondary electrons  $i_s$  to the number of primary electrons  $i_p$ ,  $\eta$  is related to  $\delta$  by the simple relation

$$\delta = \delta_{\text{true}} + \eta, \quad (5)$$

where  $\delta_{\text{true}}$  is the fractional yield consisting of 'true' secondaries (energy less than 50 eV). Following Bruining [17], who derived a relation for secondary electron emission as

$$\delta_\alpha = \delta_0 \exp[\gamma x_d (1 - \cos \alpha)] \quad (6)$$

which is also applicable to backscattering electrons, i.e.,

$$\eta_\alpha = \eta_0 \exp[\gamma x_d (1 - \cos \alpha)], \quad (7)$$

where  $\eta_\alpha$  is the backscattering coefficient at incidence angle  $\alpha$ ,  $\eta_0$  for normal incidence,  $\gamma$  is the absorption coefficient and  $x_d$  is the diffusion range [18].

Equation (7) could be used not only to see the angular dependence of  $\eta$  but also to calculate the diffusion range  $x_d$  in the material if its absorption coefficient is available as a known parameter.

**3.3.1 Experimental procedure:** A highly pure and mechanically polished thick foil of a chosen solid target is fixed on the movable target holder which can rotate with respect to the direction of incident beam. In order to measure the angular dependence of  $\eta$  for a solid target at a given impact energy, experimental arrangement and procedures are followed in the manner as they are described in detail in our recent publication [12].

While measuring the total yield  $\delta$ , the grid is kept at +50 V, thus adding all the secondaries (true secondaries + back scattering). They are collected at the monitoring plate. With the help of plate current  $i_s$  and target current  $i_t$ , the total secondary emission yield ( $\delta$ ) is calculated as

$$\delta = i_s / (i_s + i_t). \quad (8)$$

From behaviour of electrons returning from the target surface, we can understand why secondary electron-imaging has been preferred in scanning electron microscopy. Secondary electrons have low energy and can easily be collected very efficiently by positively biased detectors. This way, one may get good signal-to-noise ratio. Backscattered electrons, on the contrary, do not fulfil these conditions.

#### 4. Conclusions

Development of a new electron-recoil ion/photon coincidence setup for studying some elementary collision processes, like, electron bremsstrahlung, electron backscattering, innershell excitation and multiple ionization in collisions of keV-electrons with gaseous and solid targets is presented. Different components involved in the setup, particularly, the indigenously built units such as a TOF spectrometer, a 45°-parallel plate electrostatic analyzer and a compact multipurpose scattering chamber are discussed at length with respect to their design and fabrication aspect. A report on performance, optimization, efficiency, time resolution etc. of the ion and electron detecting systems is presented. Further, the test spectra for electron-recoil ion coincidence, ejected electron energy distribution and for X-ray spectrum from a gaseous target are produced. These examples illustrate the level of performance of the present setup and give us confidence to perform a meaningful experiment of a desired nature.

#### Acknowledgement

We thankfully acknowledge the financial support given by Department of Science and Technology (DST), New Delhi, India under the project No: SP/S2/L-17/95 and by German Research Council (DFG), Germany under INSA/DFG International Collaborative Research Program. R K Singh and R K Mohanta are grateful for receiving the financial assistance from DST during the progress of the work.

## References

- [1] K Stephan, H Helm and T D Märk, *J. Chem. Phys.* **73**, 3763 (1980)
- [2] R C Wetzel, F A Baiocchi, T R Hayes and R S Freund, *Phys. Rev.* **A35**, 559 (1987)
- [3] E Krishnakumar and S K Srivastava, *J. Phys.* **B 21**, 1055 (1988)
- [4] R Saeed, A J Duncan and H Kleinpoppen, *Phys. Rev.* **A6**, 3328 (1984)
- [5] C B Opal, E C Beaty and W K Peterson, *At. Data* **4**, 209 (1972)
- [6] M A Chaudhry, A J Duncan, R Hippler and H Kleinpoppen, *Phys. Rev. Lett.* **59**, 2036 (1987)
- [7] G H Dunn, in *Electron impact ionization* edited by T D Mark and G H Dunn (Springer Verlag, New York, 1985) p. 277
- [8] S K Goel and R Shanker, *Phys. Rev.* **A54**, 2056 (1996)
- [9] S K Goel and R Shanker, *J. X-ray Science and Technology* **7**, 331 (1997)
- [10] S K Goel, R Hippler, R K Singh and R Shanker, *Pramana – J. Phys.* **52**, 493 (1999)
- [11] R Ambrose, D L Kahler, H E Lehtihet and C A Quarles, *Nucl. Instrum. Methods Phys. Res.* **B56/57**, 327 (1991)
- [12] R K Singh and R Shanker, *J. Phys.* **D31**, 2221 (1998)
- [13] S K Goel, M J Singh and R Shanker, *Pramana – J. Phys.* **45**, 291 (1995)
- [14] M J Singh, S K Goel, R Shanker, D O Kataria, N Madhavan, P Sugathan, J J Das, D K Avasthi and A K Sinha, *Pramana – J. Phys.* **49**, 521 (1997)
- [15] G A Harrower, *Rev. Sci. Instrum.* **20**, 850 (1955)
- [16] E Storm, *Phys. Rev.* **A5**, 2328 (1972)
- [17] H Bruining, *Physica* **5**, 901 (1938)
- [18] G D Archard, *J. Appl. Phys.* **32**, 1505 (1961)